

The collimation–corrected GRB energies correlate with the peak energy of their νF_ν spectrum

Giancarlo Ghirlanda¹, Gabriele Ghisellini¹ and Davide Lazzati²

1 INAF - Osservatorio Astronomico di Brera, via Bianchi 46, 23807 Merate, Italy

2 Institute of Astronomy, Madingley Road CB3 0HA, Cambridge UK

ABSTRACT

We consider all bursts with known redshift and νF_ν peak energy, E_{peak}^{obs} . For a good fraction of them an estimate of the jet opening angle is available from the achromatic break of their afterglow light curve. This allows the derivation of the collimation–corrected energy of the bursts, E_γ . The distribution of the values of E_γ is more spread with respect to previous findings, covering about two orders of magnitude. We find a surprisingly tight correlation between E_γ and the source frame E_{peak} : $E_{peak}^{obs}(1+z) \propto E_\gamma^{0.7}$. This correlation can shed light on the still uncertain radiation processes for the prompt GRB emission. More importantly, if the small scatter of this newly found correlation will be confirmed by forthcoming data, it will be possible to use it for cosmological purposes.

Subject headings: Gamma Rays: bursts — Radiative processes: non-thermal

1. Introduction

The possibility that GRB fireballs are collimated was first proposed for GRB 970508 (Waxman et al. 1998) and subsequently invoked for GRB 990123 as a possible explanation for its extraordinarily large isotropic energy (Fruchter et al. 1999). The observational evidence supporting this scenario is the achromatic break of the afterglow light curve which declines more steeply than in the spherical case (e.g. Rhoads 1997, Sari, Piran & Halpern 1999). Under the simplifying assumption of a constant circum-burst density medium of number density n , a fireball emitting a fraction η_γ of its kinetic energy in the prompt γ -ray phase would show a break in its afterglow light curve when its bulk Lorentz factor Γ becomes of the order of $\Gamma \simeq 1/\theta$ with θ given by (Sari et al. 1999)¹:

$$\theta = 0.161 \left(\frac{t_{jet,d}}{1+z} \right)^{3/8} \left(\frac{n \eta_\gamma}{E_{\gamma,iso,52}} \right)^{1/8} \quad (1)$$

¹The notation $Q = 10^x Q_x$ is adopted, with cgs units.

where z is the redshift, $t_{jet,d}$ is the break time in days, and $E_{\gamma,iso}$ is the energy in γ -rays calculated assuming that the emission is isotropic. The collimation-corrected energy is $E_{\gamma} = (1 - \cos \theta)E_{\gamma,iso}$.

Frail et al. (2001 – F01 thereafter) considering a sample of 15 bursts with redshift and estimate of θ (including 5 lower/upper limits) found the remarkable result of a clustering of E_{γ} around 5×10^{50} erg. This was also confirmed independently by Panaitescu & Kumar (2001). More recently, Bloom et al. (2003 – B03 hereafter) found that the distribution of E_{γ} for a larger sample of 24 bursts (including 8 lower/upper limits) clusters around 1.3×10^{51} erg, emphasizing at the same time the presence of several outliers with a sizeably smaller energetics. These results suggest that GRBs are characterized by a universal energy reservoir, despite the very large range of isotropic equivalent energetics.

A correlation between $E_{\gamma,iso}$ and the source frame peak energy E_{peak} was discovered by Amati et al. (2002) (see also Lloyd-Ronning et al. 2000, Lamb et al. 2003; Sakamoto et al. 2004). An analogous correlation holds between the peak luminosity $L_{peak,iso}$ and E_{peak} (Schaefer 2003; Yonetoku et al. 2003). Possible interpretations of these correlations (Schaefer 2003; Eichler & Levinson 2004, Liang et al. 2004) are now under intense discussion. It seems therefore that the local energy content of the jet plays a crucial role in determining the typical photon energy E_{peak} . In this paper we show that the tightest correlation is instead between E_{peak} and E_{γ} .

2. Sample selection

We considered all the 40 GRBs with measured redshift up to June 2004 ².

The prompt emission spectrum of GRBs can be described by a phenomenological spectral model (i.e. the Band function, Band et al. 1993) composed by low and high energy powerlaws, with photon spectral indices α and β respectively, smoothly connected by an exponential cutoff with a characteristic energy E_{break} . In the νF_{ν} representation this model predicts a peak energy $E_{peak} = (\alpha + 2)E_{break}$. For all the bursts with measured redshift we searched in the literature any information about their prompt emission spectrum. All bursts with firm redshift measurement and published E_{peak} were included in our final sample reported in Tab. 1. This sample contains 29 GRBs detected by different instruments (Col. 1) and distributed in redshift (Col. 2) between $z=0.0085$ (GRB 980425, the second nearest is the

²A continuously updated collection of GRBs with links to the relative GCN communications can be found at <http://www.mpe.mpg.de/jcg/grbgen.html>

X-ray Flash 020903 with $z=0.25$, Soderberg et al. 2004) and $z=4.5$ (GRB 000131, Andersen et al. 2000). Col. 3 to Col. 8 report the parameters of the spectrum integrated over the burst duration (Col. 6). The average low (Col. 3) and high (Col. 4) energy spectral indices of our sample are $\langle\alpha\rangle = -1.05 \pm 0.44$ and $\langle\beta\rangle = -2.28 \pm 0.25$, which are consistent with the typical values found from the spectral analysis of bright long bursts (see, e.g. Preece et al. 2000). All the GRBs for which a redshift has been measured belong to the population of long bursts (e.g. Kouveliotou et al. 1993) and the average duration of the sample reported in Tab. 1 is 88 sec. The fluences (although not uniformly integrated over the same energy range) are representative of the typical GRB values. For the GRB detected by *BeppoSAX* and studied by Amati et al. (2002) the spectral parameters are derived combining the Wide Field Camera (WFC) and the Gamma Ray Burst Monitor (GRBM) instruments on-board *BeppoSAX*, while the fluence is given by the analysis of the GRBM data only. There is a small difference between the γ -ray fluences derived fitting the GRBM data only or the GRBM+WFC data. Therefore, using the spectral indices and the normalization obtainable from the fluences given in Tab. 1 does not lead to the correct value of $E_{\gamma,iso}$ reported in Tab. 2 (for *BeppoSAX* bursts only). The latter is taken directly from Amati et al. (2002), i.e. from the combined fit. Note also that for bright bursts the GRBM instrument is sensitive over a larger energy range (extending towards higher energy) than the nominal 40–700 keV interval.

Eight GRBs (Tab. 3) were excluded from this sample either because their redshift was uncertain (2 GRBs) or because their peak energy was not found in the literature (6 GRBs). They are discussed in Sect. 4.1 and their consistency with the conclusions drawn for the main sample is checked under reasonable assumptions for the lacking parameters.

From the original sample of 40 GRBs with known redshift only 3 cases were completely excluded from the present analysis: GRB 020124 (Ricker G. et al. 2002), whose spectral properties are reported in Barraud et al. (2003), presents a peak energy of ~ 1 MeV with an uncertainty of an order of magnitude; GRB 030323 (Graziani et al. 2003) for which no peak energy or fluence was reported in the literature and GRB 031203 (Gotz et al. 2003) without a (yet) published prompt phase spectrum.

Considering all the bursts presented in this work (Tab. 1 and Tab. 3) our sample contains 37 GRBs.

3. Isotropic energy and collimation correction

The source frame isotropic equivalent energy of a burst can be derived from its frequency and time integrated flux. If the jet opening angle is known then we can calculate the collimation corrected energy. These quantities for the sample of selected bursts are reported in Tab. 2.

Similarly to Bloom et al. (2001, 2003) and Amati et al. (2002) we derived for every burst reported in Tab. 1 the source frame “bolometric” isotropic energy $E_{\gamma,iso}$ integrating the best fit time-integrated model spectrum $N(E)$ [phot cm⁻² keV⁻¹] over the energy range 1 keV–10 MeV. The integration over such a large band also required the proper correction for the band-redshift effect so that:

$$E_{\gamma,iso} = \frac{4\pi D_l^2}{(1+z)} \int_{1/(1+z)}^{10^4/(1+z)} E N(E) dE \quad \text{erg} \quad (2)$$

where E is in keV and D_l is the source luminosity distance (we adopt $\Omega_m=0.3$, $\Omega_\Lambda=0.7$, $H_0=70$ km s⁻¹ Mpc⁻¹). Note that Amati et al. 2002 assume for the *BeppoSAX* bursts a value of $H_0 = 65$ km s⁻¹ Mpc⁻¹ in deriving $E_{\gamma,iso}$. For these bursts we corrected their $E_{\gamma,iso}$ (col. 7 in Tab. 2) for our different H_0 .

For 24/29 GRBs reported in Tab. 1 a jet break time is known and the collimation angle θ can be derived (Eq. 1). For these we used the isotropic energy estimated above with a constant energy conversion efficiency $\eta_\gamma=20\%$ (see also F01). Only in few cases the circum-burst density was measured (from broad band modeling of the afterglow emission, e.g. Panaitescu & Kumar 2001, 2002) and used in deriving θ . For those bursts with unknown n we assumed the median value $n \simeq 3$ cm⁻³ of the distribution of the measured densities which extends roughly between 1 and 10 cm⁻³ (Frail et al. 2000a, Yost et al. 2002, Panaitescu & Kumar 2002, Frail et al. 2003, Harrison et al. 2001, Schaefer et al. 2003). This density was also assumed for GRB 990123 although Panaitescu & Kumar (2001), fitting simultaneously the afterglow light curves in different bands, found for this burst and for GRB 980703 $n \simeq 10^{-3}$ cm⁻³. Studying the radio properties of GRB 980703, Frail et al. (2003) found $n \sim 30$ cm⁻³, and discussed the possible reasons for the discrepancy with the value quoted above (see also Berger et al. 2004a), which could be applied also to GRB 990123 (see also Nakar & Piran 2004). Similar to F01 and B03 we have then treated GRB 990123 as a burst with unknown circum-bursts density, and therefore used $n = 3$ cm⁻³ (note that F01 used $n = 0.1$ cm⁻³, while B03 used $n = 10$ cm⁻³).

The jet break time (collected in most cases from B03) is reported in Tab. 2 (Col. 1) for all the bursts (16) for which a direct measure of this parameter was possible from the broad band modeling of the afterglow light curve. For 7 GRBs only upper/lower limits on

t_{jet} were estimated from the available data. These limits determine the upper/lower limits on the collimation–corrected energy reported in Tab. 1 (Col. 7). On the other hand there are a handful of GRBs whose spectrum is best fit by a Band function with high energy spectral index $\beta > -2$. This indicates that E_{peak} is outside (above) the fitting energy range. These cases are reported as lower limits in energy (Tab. 2, Col. 8). Only for XRF 030723 the limit on the peak energy and on the isotropic energy is due to the limit on its redshift $z < 2.1$ (Fynbo et al. 2004).

The jet break time, the derived jet opening angle, the source frame isotropic energy $E_{\gamma,iso}$, collimation–corrected energy E_{γ} and peak energy E_{peak} are reported in Tab. 2 for the sample of bursts in Tab. 1. Tab. 4 reports these quantities for the few GRBs of Tab. 3 with uncertain parameters. We note that, due to the larger energy range for the calculation of the isotropic energy and to the slightly different circum-burst assumed density, the values of θ and E_{γ} reported in Tab. 2 are different with respect to those reported by F01 and B03 for the common GRBs.

The spectral parameters of several bursts reported in Tab. 1 (and Tab. 2) were published without the relative errors. For these parameters we assumed the average errors (in square parenthesis) obtained from those bursts with published parameters’ errors (in round parenthesis). Furthermore, we do not know the correlations among the parameters entering in the calculation of the jet opening angle and of the collimation corrected energy. For this reason (see also B03) the simplest approach is to propagate the errors in their calculations assuming that these parameters are uncorrelated. In all the tables the errors obtained with this method are reported in square parenthesis and the resulting average uncertainty on the three fundamental quantities E_{peak} , θ and E_{γ} are 20%, 32% and 20%, respectively.

4. Results

In Fig. 1 we report (*filled symbols*) the source frame peak energy $E_{peak}(1+z)$ versus the collimation corrected energy E_{γ} for the 24 GRBs with redshift and θ . We find that these two parameters are highly correlated with a Spearman’s rank correlation coefficient $r_s=0.88$ and a null hypothesis probability of being uncorrelated of 2.7×10^{-8} . If we exclude from the correlation all the bursts (8) for which either the computed E_{peak} and/or E_{γ} are upper/lower limits we derive a correlation coefficient of $r_s=0.94$ (with a probability of 1.4×10^{-7}) and the best fit powerlaw model, obtained accounting for errors on both coordinates (routine fitexy of Press et al. 1999), is (*solid line* in Fig. 1)

$$E_{peak} = 267.0 \left(\frac{E_{\gamma}}{4.3 \times 10^{50} \text{ erg}} \right)^{0.706 \pm 0.047} \text{ keV} \quad (3)$$

Note that fitting E_γ versus E_{peak} with this method gives $E_\gamma \propto E_{peak}^{1.416 \pm 0.09}$, which is exactly equivalent to Eq. 3. Fig. 1 also shows (*open symbols*), for all the 30 GRBs present in Tab. 1, the peak energy and the isotropic equivalent energy $E_{\gamma,iso}$. This correlation presents a larger spread with respect to previous findings (Amati et al. 2002, Lamb et al. 2003) due to the larger number of objects included in the sample. The correlation coefficient results $r_s=0.803$ (with a probability of 7.6×10^{-7}) and excluding the upper/lower limits on E_{peak} (3 GRBs) the best fit is $E_{peak} = 258(E_{\gamma,iso}/1.2 \times 10^{53} \text{erg})^{0.40 \pm 0.05}$ (*dashed line* in Fig. 1). Note that, especially for $E_{peak} \sim 500\text{--}600$ keV, there is a relatively large scatter of $E_{\gamma,iso}$ values around the fitting line. For the very same bursts the scatter of E_γ around the fitting $E_{peak} - E_\gamma$ line is much reduced. This means that it is possible that bursts with the same E_γ and E_{peak} have different jet opening angle.

Of all the bursts included in Tab. 1 only GRB 980425 represents an outlier for the $E_{peak} - E_{\gamma,iso}$ correlation, and for this burst the angle is unknown. Instead XRF030723 and XRF020903 are consistent with the extrapolation of the above correlation at very low peak energies (see also Lamb et al. 2003). For XRF030723 there are indications of a break in the lightcurve between 30 and 50 hours (Dullighan et al. 2003), while for XRF020903 a jet break time around 3 days (corresponding to ~ 25 days), would be required to bring it on the $E_{peak} - E_\gamma$ correlation. The 8.46 GHz data of XRF020903 presented in Soderberg et al. (2004) show a relatively fast time decay (decay index < -1.5), after the source became transparent (i.e. ~ 25 days after the trigger). However, Soderberg et al. (2004) claim that there is no sign of jet break at 4.86 GHz, where the flux increases up to ~ 30 days after the trigger. If this is the case, then XRF020903 would be an outlier.

The correlation that we find between the peak energy and the collimation corrected energy is also extremely narrow and we note that except for one burst (GRB 000911) all the upper/lower limits are still consistent with this correlation. In Fig. 2(a) we report the distribution of the isotropic energy which, similarly to what reported by many authors (Bloom et al. 2001, Frail et al. 2001, Berger et al. 2003), is wide spread over almost 3 orders of magnitude between 6.8×10^{51} erg and 2.8×10^{54} erg. Applying the correction for the collimation angle, this distribution clusters around a typical value of $\sim 10^{51}$ erg (Fig. 2(b)). The gaussian fit to the logarithmic distribution of E_γ results in a central value $\langle \log(E_\gamma) \rangle = 50.8$ with a standard deviation of 0.6. Introducing the correlation of E_γ with E_{peak} we can derive a measure of the dispersion of the GRBs around the correlation $E_{peak} \propto E_\gamma^{0.7}$ in the log-log plane. The distribution of the dispersion measure is reported in Fig. 2(c) and its average value is 0.041 ± 0.015 with a maximum logarithmic dispersion of 0.25. We note that this distribution represents the effective tight correlation between E_{peak} and E_γ .

4.1. Consistency checks

From the sample of GRBs with measured redshift we excluded 8 cases with uncertain redshift and/or peak energy. These GRBs are reported (with the same meaning of the columns) in Tab. 3. In this section we discuss their consistency with the above correlation under reasonable assumptions on their lacking parameters.

GRB 970508 was detected both by *BeppoSAX* and BATSE. According to the analysis of *BeppoSAX* data (Amati et al 2002) its peak energy should be 145 ± 43 keV whereas the analysis of the BATSE spectrum (Jimenez et al. 2001) reports an unconstrained peak energy (due to a high powerlaw spectral index $\beta > -2$). The latter determines only a lower limit of $E_{peak} > 1503$ keV (rest frame). A more difficult situation was encountered for 5 GRBs (991208, 000210, 000301C, 000418, 000926) with unpublished spectral parameters. Except for GRB991208, the other events were detected by one of the satellites of the Interplanetary Network. These instruments are most likely sensitive to GRBs with a spectrum similar to that of bursts detected by BATSE. For this reasons, having only a fluence, we assumed a typical Band function with α and β equal to the average values of these parameters for the bursts presented in Tab. 1 (see also sec.2) and with a break energy free to vary in the range 100-500 keV which is a conservative estimate of the typical width of the distribution of this spectral parameter for BATSE bright bursts (Preece et al. 2000). With the above assumptions we iteratively calculated $E_{\gamma,iso}$, E_{peak} and E_{γ} for these bursts and report their interval of variation in Fig. 3. In Tab. 4 we report for reference their peak energy, isotropic equivalent energy and collimation corrected energy corresponding to the assumption of the above average spectrum with break energy equal to the central value of its allowed range of variation.

Finally there are two GRBs (980326 and 980329) with uncertain redshift measurements. There are some indications (Bloom et al. 1999) that 980326 lies at $z < 1.5$ (this limiting value was assumed by B03) and that 980329 might be between redshift 2 and 3.9. For these two events we calculated the region of the $E_{peak}-E_{\gamma,iso}, E_{\gamma}$ plane were they lie varying their z within these ranges. They are represented by the connected polygons in Fig. 3. In Tab. 4 we report for these two cases the parameters obtained assuming the median values (i.e. 1.0 and 3.0) of the ranges where their redshift was allowed to vary.

We can see from Fig. 3 that with the above reasonable assumptions on the uncertainty of their spectral parameters or distance also these 8 GRBs are still consistent with the found correlation between E_{peak} and E_{γ} .

5. Discussion

The analysis of a sample of GRBs with measured redshift and peak energy revealed a tight correlation between their peak spectral energy and collimation corrected energy:

$$E_{peak} \simeq 480 \left(\frac{E_\gamma}{10^{51}\text{erg}} \right)^{0.7} \text{ keV} \quad (4)$$

The maximum (logarithmic) scatter from this correlation in the sample of 24 GRBs with measured jet opening angle is ~ 0.25 dex while its distribution (Fig. 2(c), insert) has a standard deviation of less than 0.1 dex.

The distribution of the collimation–corrected energy (Fig. 2(b)) for our GRB sample presents a wider spread compared to the same distribution in F01 and B03. This is due to the different energy bands in which the E_γ has been computed and to the fact that our sample includes several recent HETE-2 GRBs not present in the B03 sample (nor obviously in the F01 one). Nevertheless the central value of our distribution $\sim 6 \times 10^{50}$ erg is consistent with what reported in F01. The tight correlation of Eq. 4 can be found in both the F01 and the B03 samples, even though the peak energy range is smaller and therefore the statistical significance lower.

We derived the jet opening angle (Eq. 1) within the framework of the standard afterglow theory (Sari et al. 1999). The small scattering around the correlation between E_{peak} and E_γ can be seen as an *a-posteriori* check that the assumptions we made are correct. This indicates that the circum-burst density, its radial profile and the efficiency coefficient η_γ are fairly standard.

We have checked that no burst among the 8 cases reported in Tab. 3 and Tab. 4, for which we have only a partial knowledge of the relevant parameters, contradicts the correlation (Fig. 3). One X–ray flash with known redshift (020903) could be consistent with our correlation assuming a jet opening angle $\theta \sim 25^\circ$. The existing radio data are controversial and this XRF could be an outlier. The other XRF in our sample (030723) lies on our correlation if its redshift is not much smaller than unity. Concerning the two GRBs associated with a SN, we have that GRB 980425/SN1998bw (Galama et al. 1998) has a very low isotropic energy and no jet break and it is standing alone with respect to any other GRB in the $E_{peak}-E_\gamma, E_{\gamma,iso}$ plane. On the other hand GRB 030329/SN2003dh (Stanek et al. 2003) with a jet opening angle of $\sim 5^\circ$ (Price et al. 2003a, Tiengo et al. 2003, Berger et al. 2004) has a collimation corrected energy and a peak spectral energy which place on the $E_{peak}-E_\gamma$ correlation.

The sample of 29 GRBs (Tab. 1, 2) also allowed to re–consider the correlation between the isotropic equivalent energy $E_{\gamma,iso}$ and the peak energy E_{peak} found by Amati et al. (2002;

see also Lloyd-Ronning et al. 2000, Lamb et al. 2003; Sakamoto et al. 2004). Including all GRBs with measured redshift (Tab. 1) we confirm the existence of such correlation. However, we find two differences. On the one hand the spread around the best correlation line is larger than previously estimated with smaller samples. On the other hand, the slope of the correlation seem to depend on whether XRFs are included or not. We find that considering only GRBs, the relation is $E_{peak} \propto E_{\gamma,iso}^{0.40 \pm 0.05}$, flatter than previously estimated, shown with a *dashed line* in Fig. 1 (see also Amati 2004, who finds a slope 0.45 ± 0.06). If instead, following Lamb et al. (2003), we include X-ray flashes, the original Amati et al. (2002) result fits better the data (*dot-dashed line* in Fig. 1). The paucity of GRB/XRFs with peak energies in the tens of keV range does not allow us to draw any firm conclusion (note that the two slopes are consistent at the $2-\sigma$ level).

The different slopes of the $E_{peak}-E_{\gamma,iso}$ (Amati et al. 2002) and the $E_{peak}-E_{\gamma}$ correlations imply that they will intersect at some small value of $E_{\gamma} = E_{\gamma,iso}$ (see Fig.1). The precise value of the intersection depends mainly on the uncertainties in the $E_{peak}-E_{\gamma,iso}$ relation, as illustrated in Fig. 1 (dashed and dot-dashed lines). At any rate, bursts lying in this region of the $E_{peak}-E_{\gamma} \sim E_{\gamma,iso}$ plane would be characterized, on average, by a nearly isotropic emission, small peak energies (possibly in the UV/soft-X-ray range) and by E_{γ} smaller than 10^{47} erg³.

Recently, it has also been shown (Liang et al. 2004) that the correlation between E_{peak} and $E_{\gamma,iso}$ (found from the time-averaged spectrum) holds when considering the time resolved spectral analysis of GRBs. Similarly, due to the much lower scatter (a factor ~ 5.7 lower) around the E_{peak} and E_{γ} correlation, we expect that considering the time resolved spectral peak energy $E_{peak}(t)$ and collimation corrected energy $E_{\gamma}(t)$ a possibly even less scattered correlation should hold within single GRBs. This, in turn, might help in exploring the (still obscure) origin of the prompt emission. In fact, although we do not have an interpretation of the found $E_{peak}-E_{\gamma}$ correlation, we believe it indicates that there should be some connection between the energy emitted by the burst and the emission process which determines its spectral properties.

The existence of the above correlation also allows to predict the jet break time, once the spectrum and the redshift of a burst are known. In the forthcoming Swift era this might contribute in optimizing the GRB follow up with planned observations at the expected jet break time. For this reason we think that it is important that the information about the peak energy be disseminated promptly together with the other fundamental GRB properties

³Note that GRB 980425 is an outlier whether or not its γ -ray emission was isotropic.

such as the position, peak flux etc. Now this routinely occurs for HETE II bursts⁴, and it is crucial that this will happen also for the future Swift bursts.

Berger et al. (2004a) recently discussed the possibility that the real standard energy in cosmic explosions (including GRBs, XRFs and hypernovae) is the total released kinetic energy rather than the fraction that goes into γ -ray photons. This energy includes corrections due to mildly relativistic material (estimated from radio emission such as in SN1998bw; Kulkarni et al. 1998) and to a longer time-scale activity of the engine (estimated from the afterglow lightcurve, such as in GRB 030329). While not in contrast with this idea, our findings underline the fact that the γ -ray energetics is still an important parameter for understanding the physics of GRBs. The found correlation implies that the peak energy of the spectrum, which is a quantity set by local micro-physical processes, is determined by a global property of the jet, namely its total γ -ray energy (or the jet opening angle).

Last but not least, the $E_{peak}-E_\gamma$ relation that we presented in this work and the low scatter of the sample of bursts with known redshifts around it strongly reminds a similar relation found for SN Ia between their luminosity and the stretching factor of their optical light curve (e.g. Phillips 1993, Perlmutter et al. 1998) with less luminous supernovae showing a faster post-maximum light curve decay (Riess et al. 1995). The proper modelling of this effect (e.g. Hamuy et al. 1996, Perlmutter et al. 1998) allows to better determine the SN luminosity and consequently reduce the scatter in the Hubble diagram with respect to the case that assumes that all SN Ia are standard candles. Similarly, our result shows that among GRBs the existence of a correlation with small scatter between their peak spectral energy and the collimation corrected energy might be used to determine the different luminosities of different bursts. The small scatter around the rest frame $E_{peak}-E_\gamma$ correlation might be used to reduce the scatter of the GRB-Hubble diagram (Bloom et al. 2003, Schaefer et al. 2003) and constrain the cosmological parameters (Ghirlanda et al. (2004) in preparation). If our relation will be confirmed and possibly extended (particularly to low peak energies) with new bursts detected by Swift, we might be able to test the cosmological models farther out the predicted SNAP SN limit of $z=1.7$ (e.g Aldering et al. 2002). This is particularly interesting since we might be able to explore an epoch in which the universe, matter dominated, was decelerating.

⁴<http://space.mit.edu/HETE/Bursts/>

6. Conclusions

We considered all the bursts with measured redshift and spectral peak energy up to now (June 2004). We systematically derived their source frame bolometric isotropic equivalent energy and, when available from the afterglow modeling (24/38), corrected this energy for their collimation angle. We found a very tight correlation between the source frame E_{peak} (the peak in the νF_ν spectrum of the prompt emission) and the collimation corrected emitted energy: $E_{peak} \sim 480 (E_\gamma/10^{51}\text{erg})^{0.7}$ keV.

- The small dispersion around this correlation is an indication of the robustness of the afterglow theory on which the estimate of the jet opening angle is based (Eq. 1, Sari et al. 1999)
- We found that, differently from previous results, GRBs do not cluster around a unique value of their collimation corrected energy, but are spread in a relatively large range (~ 2 orders of magnitudes) centered at $E_\gamma \sim 6 \times 10^{50}$ erg. We believe that the smaller spread found previously around a similar value $\sim 5 \times 10^{50}$ erg (Frail et al. 2001, Bloom et al. 2003, Panaitescu & Kumar 2001) might be the result of a limited sample of GRBs within a relatively small E_{peak} range.
- The underlying physical motivation of the correlation is mysterious, but it is likely that it is the result of the radiation process producing the prompt emission which should be related to the local energy content of the burst.
- There are relatively few bursts with $10 < E_{peak} < 100$ keV, just the range of the BAT instrument on-board Swift, which therefore will be crucial for confirming or discarding the correlation.
- Finally, and more importantly, the correlation (if the small scatter around it will be confirmed) makes GRBs exquisite cosmological tools, to measure Ω_m, Ω_Λ in a redshift range not accessible to Supernovae Ia, that is, $z > 1.7$, and up to any redshift. Even if the optical information is unavailable for $z > 2.5$, the necessary information about the jet break time can be gathered by following the X-ray and/or the IR afterglow. Partial obscuration by dust, which can be an issue for using Supernovae as standard candles, does not influence GRBs.

We thank the referee for her/his comments which improved the paper and Annalisa Celotti for useful discussions. DL thanks the Osservatorio Astronomico di Brera for the kind hospitality during part of the preparation of this work. G. Ghirlanda thanks the ASI (/I/R/390/02) for financial support. We thank M. R. Panzera for technical support.

REFERENCES

- Aldering, G. et al. 2002, SPIE, 4835, 146
- Amati, L. et al. 2000, Sci, 290, 953
- Amati, L. et al., 2002, A&A, 390, 81
- Amati, L. et al., 2004, preprint (astro-ph/0405318)
- Atteia, J.-L. et al. 2003, A&A, 407, L1
- Andersen, M. I. et al. 2000, A&A, 364, L54
- Andersen, M. I. et al. 2003, GCN, 1993
- Antonelli, L. A. et al. 2000, ApJ, 545, L39
- Barraud, C. et al. 2003, A&A, 400, 1021
- Berger, E. et al. 2003, ApJ., 590, 379
- Berger, E. et al. 2004, Nat, 426, 154
- Berger, E. et al. 2004a, preprint (astro-ph/0405431)
- Berger, E. et al. 2004b, GCN, 2599
- Bersier, D. et al. 2004, GCN, 2602
- Bloom, J. S. et al. 1999, Nat., 401, 453
- Bloom, J. S., Frail, D.A. & Kulkarni, S.R. 2003, ApJ, 594, 674
- Bloom, J. S. et al. 2002, GCN, 1452
- Bloom, J. S., Frail D. A. & Sari R. 2001, Astron. J., 121, 2879
- Bjornsson G., et al. 2001, ApJ, 552, L121
- Burenin, R. et al. 2003, GCN, 1990
- Castro S. M. et al. 2000, GCN, 605
- Castro S. M. et al. 2000a, GCN, 851
- Crew, G. B. et al. 2003, ApJ, 599, 387

Della Valle, M. et al. 2003, A&A, 406, L33
Djorgovsky, S. G. et al. 1998a, GCN, 189
Djorgovsky, S. G. et al. 1998b, GCN, 137
Djorgovsky, S. G. et al. 1998c, GCN, 289
Djorgovsky, S. G. et al. 2001, ApJ, 526, 654
Djorgovski, S. G. et al. 2001a, GCN, 1108
Dodonov, S. N. et al. 1999, GCN, 461
Dulligan, A. et al. 2004, GCN, 2588
Dulligan, A. et al. 2003, GCN, 2336
Frail, D. A. et al., 2001, ApJ, 562, L55 (F01)
Frail, D. A. et al., 2003, ApJ, 590, 992
Fruchter, A. et al. 1999, ApJ, 519, L13
Fruchter, A. et al. 2001, GCN, 1200
Fynbo, J. P. U. et al. 2004, GCN, 2327
Galama, T. J. et al. 1998, Nat., 396, 670
Galama, T. J. et al. 1999, GCN, 338
Garnavich, P. M. et al. 2000 ApJ, 544, L11
Gorosabel, J. et al. 2002, GCN, 1224
Gotz, D. et al. 2003, GCN, 2459
Greiner, J. et al. 2002, GCN, 1886
Greiner, J. et al. 2003, GCN, 2020
Graziani, C. et al. 2003, GCN, 1956
Hamuy, M. et al. 1996, ApJ, 112, 6
Harrison, D. L. et al. 2001, ApJ, 599, 123

- Hjorth, J. et al. 2003, ApJ, 597, 699
- Hjorth, J. 1999, GCN, 219
- Hurley, K. et al. 2000, GCN, 642
- Hurley, K. et al. 2000a, GCN, 802
- Infante, L. et al. 2001, GCN, 1152
- Israel, G. L. et al. 1999, A&A, 348, L5
- Jakobsson, S. P. et al. 2003, A&A, 408, 941
- Jakobsson, S. P. et al. 2004, A&A, in press (astro-ph/0407439)
- Jimenez, R., Band, D. L. & Piran, T., 2001, ApJ, 561, 171
- Klose, S., et al., 2004, AJ submitted
- Kouveliotou, C. et al. 1993, ApJ, 413, L101
- Kulkarni, S. et al. 1998, Nat, 393, 35
- Lamb, D.Q. et al. 2003, preprint (astro-ph/0312634)
- Liang, E. W., Dai Z. G. and Wu X. F. 2004, ApJ, 606, L29
- Linder, E. V. 2003, AIPC, 655, L193
- Lloyd, M. N., Petrosian V., Mallozzi R. S. 2000, ApJ, 534, L227
- Masetti, N. et al. 2002, GCN, 1330
- Metzger, M. R. et al. 1997, Nat., 387, 878
- Nakar, E. & Piran T. 2004, preprint (astro-ph/0405473)
- Panaitescu, A. & Kumar, P., 2001, ApJ, 554, 667
- Pandey, S. B. et al. 2004, A&A, 417, 919
- Perlmutter, S. et al. 1999, ApJ, 517, 565
- Perterson, B. A. & Price P. A. 2003, GCN, 1974
- Phyllips, M. M. 1993, ApJ, 413, L105

- Piran, T. et al. 2000, 5th Hunt. Symp., p.87
- Piro, L. et al. 2004 in preparation
- Press, W. H., Teukolsky, S. A., Vetterling, W. T. and Flannery, B. P., 1999, Numerical Recipes in C, p. 668
- Price, P.A. et al. 2002, ApJ, 573,85
- Price, P.A. et al. 2002a, GCN 1475
- Price, P.A. et al. 2003, ApJ, 589, 838
- Price, P.A. et al. 2003a, Nat, 423, 844
- Ricker, G. et al. 2002, GCN, 1220
- Riess, A. G. et al. 1995, ApJ, 438, L17
- Rol, E. et al. 2003, GCN, 1981
- Sari R. 1999, ApJ, 524, L43
- Schaefer, B. E. et al. 2003, ApJ, 583, L67
- Soderberg, A. M. et al. 2004, GCN, 1554
- Soderberg, A. M. et al. 2004, ApJ, 606, 994
- Stanek, K. Z. et al. 2003, ApJ, 519, L17
- Stanek, K. Z. et al. 2001, IAUC, 7586
- Stornelli, M. et al. 2000, GCN, 540
- Tiengo, A. et al. 2003, A&A, 409, 938
- Tinney, C. et al. 1998, IAUC, 6896
- Torii, T. et al. 2002, GCN, 1378
- Vanderspek, R. et al. 2004, preprint (astro-ph/0401311)
- Vreeswijk, P.M. et al. 1999, GCN, 324
- Vreeswijk, P. M. et al. 1999a, GCN, 496

Vreeswijk, P. M. et al. 2003, GCN, 1785

Weidinger, M. et al. 2003, GCN, 2215

Yost, S. A. et al. 2002, ApJ, 577, 155

Table 1. Sample of GRBs

GRB ^a	z^b	α	β	E_{peak} (keV) ^c	T ₉₀ (s)	Fluence (erg/cm ²)	Range (keV)	ref ^d
970228 S/B	0.695 (H)	-1.54 (0.08)	-2.5 (0.4)	115 (38)	80	1.1e-5 (0.1)	40-700	(1),(31)
970828 R/A(B)	0.957 (H)	-0.70 [0.08]	-2.07 [0.37]	298 [59]	146.59	9.6e-5 [0.9]	20-2000	(2),(32)
971214 S/B	3.42 (H)	-0.76 (0.1)	-2.7 (1.1)	155 (30)	35	8.8e-6 (0.9)	40-700	(3),(31)
980425 B/S	0.0085 (H)	-1.266 [0.13]	...	118 [24]	37.41	3.8e-6 [0.4]	20-2000	(4),(32)
980613 S	1.096 (H)	-1.43 (0.24)	-2.7 (0.6)	93 (43)	20	1.0e-6 (0.2)	40-700	(5),(31)
980703 R/A(B)	0.966 (O)	-1.31 [0.14]	-2.39 [0.26]	255 [51]	102.37	2.3e-5 [0.2]	20-2000	(6),(32)
990123 S/B	1.6 (O)	-0.89 (0.08)	-2.45 (0.97)	781 (62)	100	3.0e-4 (0.4)	40-700	(7),(31)
990506 B	1.3066	-1.37 [0.15]	-2.15 [0.38]	283 [57]	220.38	1.9e-4 [0.2]	20-2000	(8),(32)
990510 S/B	1.619 (O)	-1.23 (0.05)	-2.7 (0.4)	163 (16)	75	1.9e-5 (0.2)	40-700	(9),(31)
990705 S	0.843 (XP,H)	-1.05 (0.21)	-2.2 (0.1)	189 (15)	42	7.5e-5 (0.8)	40-700	(10),(31)
990712 S	0.43 (O,H)	-1.88 (0.07)	-2.48 (0.56)	65 (11)	20	6.5e-6 (0.3)	40-700	(11),(31)
991216 B	1.02 (O)	-1.234 [0.13]	-2.18 [0.39]	318 [64]	24.9	1.9e-4 [0.2]	20-2000	(12),(32)
000131 B	4.5 (H)	-0.688 [0.08]	-2.07 [0.37]	130 [26]	110.1	4.2e-5 [0.4]	20-2000	(13),(32)
000214 S	0.42(XP)	-1.62 (0.13)	-2.1	>82	10	1.4e-5 (0.04)	40-700	(14),(31)
000911 I	1.058 (H)	-1.11 [0.12]	-2.32 [0.41]	579 [116]	500	2.2e-4 [0.2]	15-8000	(15),(33)
010222 S	1.473 (O)	-1.35 (0.19)	-1.64 (0.02)	>358	130	9.3e-5 (0.3)	40-700	(16),(31)
010921 H	0.45 (H)	-1.49 [0.16]	-2.3	106 [21]	24.6	1.0e-5 [0.1]	30-700	(17),(34,35)
011121 S	0.36 (O) (>-2)	>700	75.	1.0e-4 [0.1]	40-700	(18),(36)
011211 S	2.14 (O)	-0.84 (0.09)	...	59 (7)	(19),(31)
020124 H	3.2 (O)	-1. [0.11]	-2.3 [0.41]	110 [22]	78.6	6.8e-6 [0.7]	30-400	(20),(35)
020405 I/S	0.69 (O)	-0.0 (0.25)	-1.87 (0.23)	364 [73]	60	7.4e-5 [0.7]	15-2000	(21),(37)
020813 H	1.25 (H)	-1.05 [0.11]	-2.3	211 [42]	90.	1.0e-4 [0.1]	30-400	(22),(34,35)
020903X H	0.25 (H)	5.52	(23),(34)
021211 H	1.01 (O)	-0.85 [0.09]	-2.37 [0.42]	47 [9]	2.41	2.2e-6 [0.2]	30-400	(24),(38)
030226 H	1.98 (O)	-0.95 [0.10]	-2.3	108 [22]	76.8	6.4e-6 [0.6]	30-400	(25),(34,35)
030328 H	1.52 (O)	-1.0 [0.11]	-2.3	110 [22]	140	2.6e-5 [0.2]	30-400	(26),(34,35)
030329 H	0.1685 (O)	-1.26 (0.02)	-2.28 (0.05)	68 (2)	23.	1.1e-4 [0.1]	30-400	(27),(39)
030429 H	2.66 (O)	35 [7]	10.3	3.8e-7 [0.3]	30-400	(28),(40)
030723X H	< 2.1	4.8	(29),(41)

^dIn round parenthesis are reported errors actually measured; when these are unavailable we assume the errors reported in square parenthesis.

^aInstrument(s) that were triggered by the GRB: S=*Beppo*SAX; B=BATSE; (B)=also BATSE, R=RXTE, A=ASM, I=IPN (Ulysses, NEAR, Konus), H=Hete-II. X-Ray Flashes (XRF) are indicated with the symbol X.

^bRedshift determined from: H=Host Galaxy spectrum; XP=X-Ray Photometric data; O=Optical Transient.

^cObserved peak energy.

^dReferences given in order for: redshift, spectral informations.

References. — (1) Djorgovsky et al. 1998; (2) Djorgovsky et al. 2001; (3) Kulkarni et al. 1998; (4) Tinney et al. 1998; (5) Djorgovsky et al. 1998a; (6) Djorgovsky et al. 1998b; (7) Hjorth 1999; (8) Bloom et al. 2001; (9) Vreeswijk et al. 1999; (10) Amati et al. 2000; (11) Galama et al. 1999; (12) Vreeswijk et al. 1999a; (13) Andersen et al. 2000; (14) Antonelli et al. 2000; (15) Price et al. 2002; (16) Stanek et al. 2001; (17) Djorgovski et al. 2001a; (18) Infante et al. 2001; (19) Amati 2004; (20) Hjorth et al. 2003; (21) Masetti et al. 2002; (22) Price et al. 2002a; (23) Soderberg et al. 2004; (24) Vreeswijk et al. 2003; (25) Greiner et al. 2002; (26) Rol et al. 2003; (27) Greiner et al. 2003; (28) Weidinger et al. 2003; (29) Fynbo et al. 2004; (30) Berger et al. 2004b; (31) Amati et al. 2002; (32) Jimenez et al. 2001; (33) Price et al. 2002; (34) Barraud et al. 2003; (35) Atteia et al. 2003; (36) Piro et al. 2004; (37) Price et al. 2003; (38) Crew et al. 2003; (39) Vanderspek et al. 2004; (40) <http://space.mit.edu/HETE/Bursts/>; (41) Lamb et al. 2003

Table 2. Sample of GRBs

GRB	t_{jet} (days)	n (cm^{-3})	ref ^a	θ (deg)	$E_{\gamma,iso}$ (erg)	E_{γ} (erg)	$E_{peak}(1+z)$ (keV)
970228,...	...	1.60e52 (0.12)	...	195 (64)
970828	2.2 (0.4)	3.0 [1-10]	(1),...	5.9 [0.8]	2.96e53 [0.35]	1.6e51 [0.5]	583 [116]
971214	>2.5 [0.4]	3.0 [1-10]	(1),...	>4.77	2.11e53 (0.24)	>7.29e50	685 (133)
980425,...	...	1.6e48 [0.2]	119 [24]
980613	>3.1	3.0 [1-10]	(1),...	>10.69	6.9e51 (0.95)	>1.0e50	194 (89)
980703	3.4 (0.5)	28 (10)	(1),(1)	11 [0.8]	6.9e52 [0.82]	1.27e51 [0.24]	502 [100]
990123	2.04 (0.46)	3.0 [1-10]	(1),...	3.98 [0.57]	2.39e54 (0.28)	5.76e51 [1.8]	2030 (161)
990506,...	...	9.49e53 [1.13]	...	653 [130]
990510	1.6 (0.2)	0.29 (0.1)	(15),(1)	3.74 [0.24]	1.78e53 [0.19]	3.79e50 [0.63]	423 (42)
990705	1.0 (0.2)	3.0 [1-10]	(1),...	4.78 [0.66]	1.82e53 (0.23)	6.33e50 [1.92]	348 (28)
990712	1.6 [0.2]	3.0 [1-10]	(2),...	9.47 [1.2]	6.72e51 (1.29)	9.16e49 [2.9]	93 (15)
991216	1.2 (0.4)	4.7 (2.3)	(1),(1)	4.4 [0.6]	6.75e53 [0.81]	2.0e51 [0.6]	641 [128]
000131	<3.5	3.0 [1-10]	(1),...	<3.8	1.84e54 [0.22]	<4.04e51	714 [142]
000214,...	...	8.0e51 (0.26)	...	>117
000911	<1.5	3.0 [1-10]	(3),...	<4.4	8.8e53 [1.05]	<2.6e51	1190 [238]
010222	0.93 (0.1)	1.7 [0.18]	(1),(1)	3.03 [0.14]	1.33e54 (0.15)	1.85e51 [0.27]	>886
010921	<33.	3.0 [1-10]	(1),...	<28.26	9.0e51 [1.0]	<1.e51	153 [31]
011121	>7	3.0 [1-10]	(1),...	>13.21	4.55e52 [0.54]	>1.2e51	>952
011211	1.5 (0.15 ^b)	3.0 [1-10]	(4),...	5.2 [0.63]	6.3e52 (0.7)	2.5d50 [0.69]	186 (24)
020124	3. [0.4]	3.0 [1-10]	(5),...	5.0 [0.3]	3.02e53 [0.36]	1.1e51 [0.32]	503 [100]
020405	1.67 (0.52)	3.0 [1-10]	(1),...	6.4 [1.05]	1.1e53 [0.13]	6.8e50 [2.39]	612 [122]
020813	0.43 (0.06)	3.0 [1-10]	(1),...	2.7 [0.13]	8.e53 [0.96]	8.8e50 [2.5]	474 [95]
020903X,...	...	2.3e49	...	<6.3
021211	>1	3.0 [1-10]	(6),...	>6.57	1.1e52 [0.13]	>7.2e49	94 [19]
030226	0.84 (0.1)	3.0 [1-10]	(12),(7)	3.94 [0.49]	1.2e53 [0.13]	2.83e50 [0.77]	322 [64]
030328	0.8 [0.1]	3.0 [1-10]	(8),...	3.7 [0.46]	2.8e53 [0.33]	5.9e50 [1.6]	277 [55]
030329	0.5 (0.1)	1 [0.11]	(9),(10)	5.1 [0.4]	1.8e52 [0.21]	7.1e49 [1.4]	79 (3)
030429	1.77 (1.0)	3.0 [1-10]	(13),...	5.96 [1.43]	2.19e52 [0.26]	1.2e50 [0.59]	128 [26]
030723X	1.67 [0.3]	3.0 [1-10]	(14),...	>10.6	<2.16e50	<4.0e48	<15

^aReferences given in order for: jet break time, external medium density

^bWe have assumed that the error is 10% instead of the 1.3% error quoted in Jakobsson et al. 2003.

References. — (1) Bloom et al. 2003 (references therein); (2) Bjornsson et al. 2001; (3) Price et al. 2002; (4) Jakobsson et al. 2003; (5) Torii et al. 2002, Gorosabel et al. 2002, Bloom et al. 2002; (6) Della Valle et al. 2003; (7) Pandey et al. 2004; (8) Andersen et al. 2003; Perterson & Price 2003, Burenin et al. 2003; (9) Berger et al. 2004; (10) Tiengo et al. 2003; (11) Bersier et al. 2004.; (12) Klose et al. 2004; (13) Jakobsson et al. 2004; (14) Dulligan et al. 2003 ; (15) Israel et al. 1999

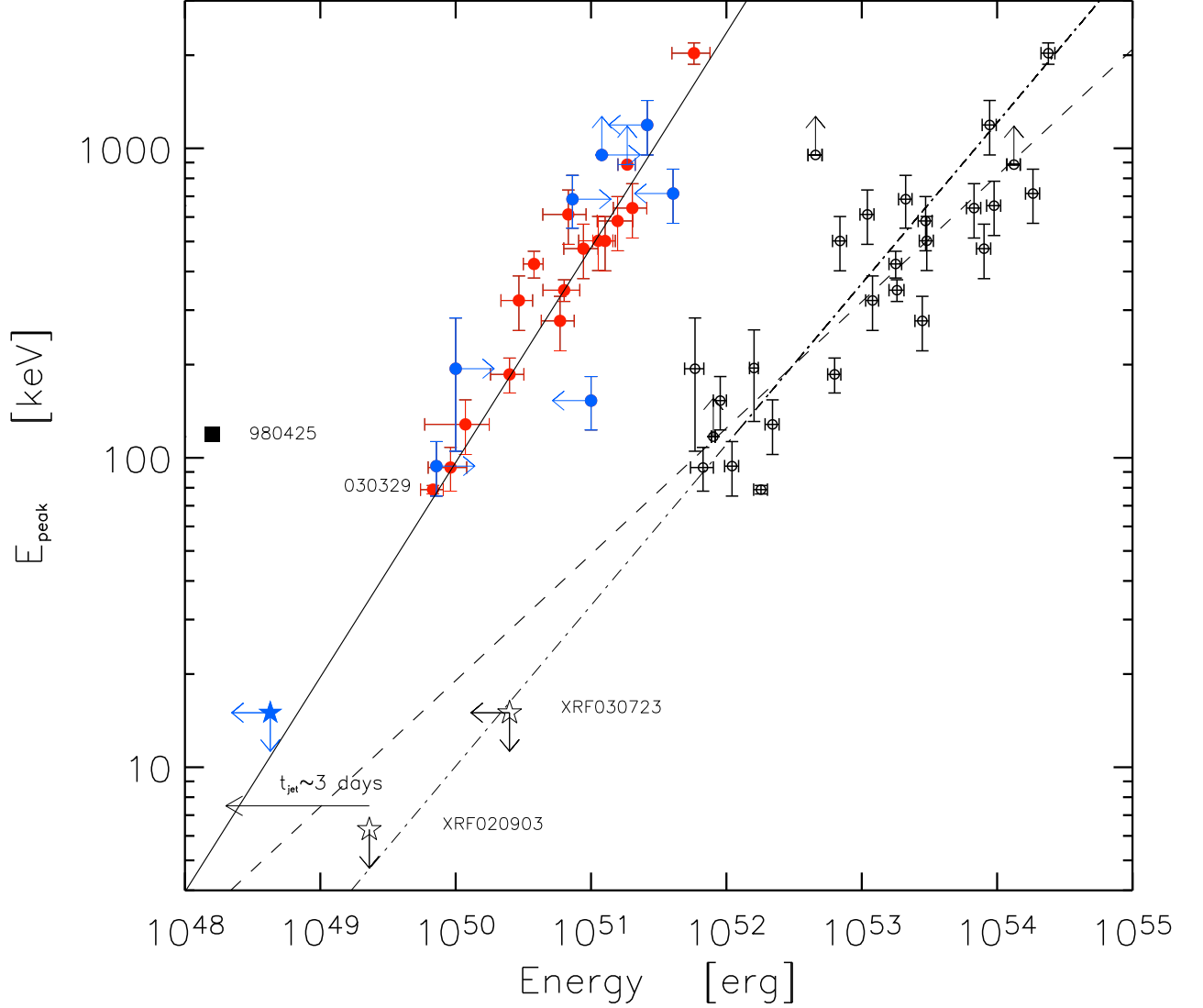


Fig. 1.— Rest frame peak energy $E_{peak} = E_{peak}^{obs}(1+z)$ versus bolometric energy for the sample of GRBs with measured redshift reported in Tab. 1. *Filled circles*: isotropic energy corrected for the collimation angle by the factor $(1-\cos\theta)$, for the events for which a jet break in the light curve was observed (see Tab. 2). Grey symbols corresponds to lower/upper limits. The *Solid line* represents the best fit to the correlation, i.e. $E_{peak} \sim 480 (E_{\gamma}/10^{51}\text{erg})^{0.7}$ keV. *Open circles*: isotropic equivalent energy $E_{\gamma,iso}$ for the GRBs reported in Tab. 2. The *Dashed line* is the best fit to these points and the *dash-dotted line* is the correlation reported by Amati et al. (2002).

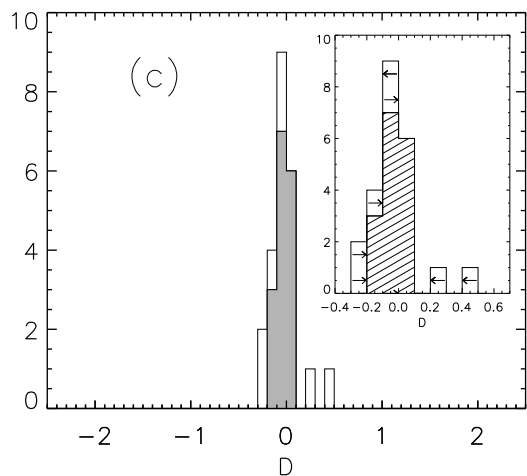
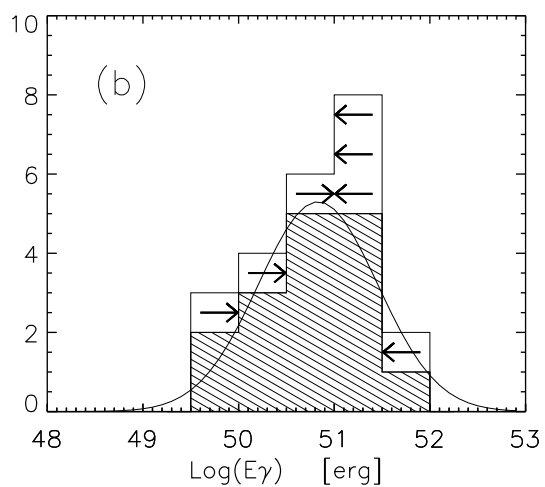
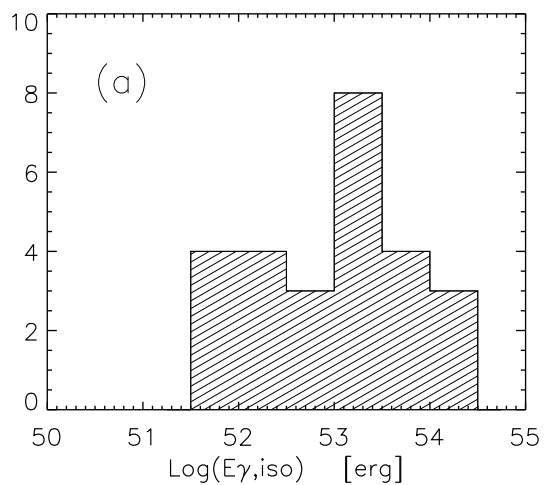


Fig. 2.— Top: distribution of the rest frame isotropic equivalent energy $E_{\gamma,iso}$ for the sample of GRBs presented in Tab. 1. Middle: Distribution of the collimation-angle corrected energy E_{γ} . Bottom: distribution of the distance of each GRB from the correlation between E_{peak} and E_{γ} . Inset: distribution of the distance from the correlation with upper and lower limits

Table 3. Uncertain cases

GRB ^a	z	α	β	E_{peak} (keV) ^d	T ₉₀ (s)	Fluence (erg/cm ²)	Range (keV)	ref ^c
970508 S/B	0.835	-1.71 (0.1)	-2.2 (0.25)	79 (23)	20	1.8e-6 (0.3)	40-700	(1),(7)
		-1.19	-1.83	> 1800		5.5e-6 [0.5]	20-2000	..., (8)
980326 S/B	...	-1.23 (0.21)	-2.48 (0.31)	33.8 (17.1)	9	0.75e-6 (0.15)	40-700	..., (7)
980329 S/B	...	-0.64 (0.14)	-2.2 (0.8)	233.7 (37.5)	25	6.5e-5 (5)	40-700	..., (7)
991208 I	0.7	60	1.e-4	25-1.e4	(2),(9)
000210 S	0.846	20	6.1e-5	2-700	(3),(10)
000301C I	2.033	50	4.1e-6	25-1.e4	(4),(11)
000418 I	1.118	30	2.e-5	15-1.e4	(5),(12)
000926 I	2.036	25	2.2e-5	25-1.e4	(6),(13)

^aInstrument(s) that were triggered by the GRB: S=*BeppoSAX*; B=*BATSE*; (B)=also *BATSE*, R=*RXTE*, A=*ASM*, I=*IPN* (*Ulysses*, *NEAR*, *Konus*).

^cReferences given in order for: redshift, spectral informations

^dObserved Peak energy

References. — (1) Metzger 1997; (2) Dodonov et al. 1999; (3) Piro et al. 2002; 4) Castro 2000; (5) Bloom et al. 2000; (6) Castro 2000a; (7) Amati et al. 2002; (8) Jimenez et al. 2001; (9) Piran et al. 2000; (10) Stornelli et al. 2000; (11) Garnavich et al. 2000; (12) Hurley et al. 2000; (13) Hurley et al. 2000a.

Table 4. Uncertain cases

GRB ^a	t_{jet} (days)	n (cm ⁻³)	ref ^e	θ (deg)	$E_{\gamma,iso}$ (erg)	E_{γ} (erg)	$E_{peak}(1+z)$ (keV)
970508	25 (5)	3.0 [1-10]	(1),...	24.0 [3.3]	7.1e51 (0.15)	6.1e50 [1.6]	145 [43]
	25 (5)	3.0 [1-10]	(1),...	22.1 [3.05]	1.4e52 [0.17]	1.02e51 [0.3]	>1503
980326	<0.4	3.0 [1-10]	(1),...	<5.08	5.6e51 (1.1)	<2.2e49	71 [36]
980329	<1	20 [10]	(1),(1)	<3.33	2.1e54 (0.2)	<3.5e51	935 (150)
991208	<2.1	3.0 [1-10]	(1),...	<8.64	1.1e53	<1.2e51	...
000210	>1.7	3.0 [1-10]	(1),...	>5.76	2e53	>1e51	...
000301C	7.3(0.5)	27 (5)	(1),(1)	13.14	4.37e52	1.14e51	...
000418	25 (5)	27	(1),(1)	22.3	7.51e52	5.6e51	...
000926	1.8(0.1)	27 (3)	(1),(1)	6.19	2.7e53	1.6e51	...

^aReferences given in order for: jet break time and external medium density.

References. — (1) Bloom et al. 2003.

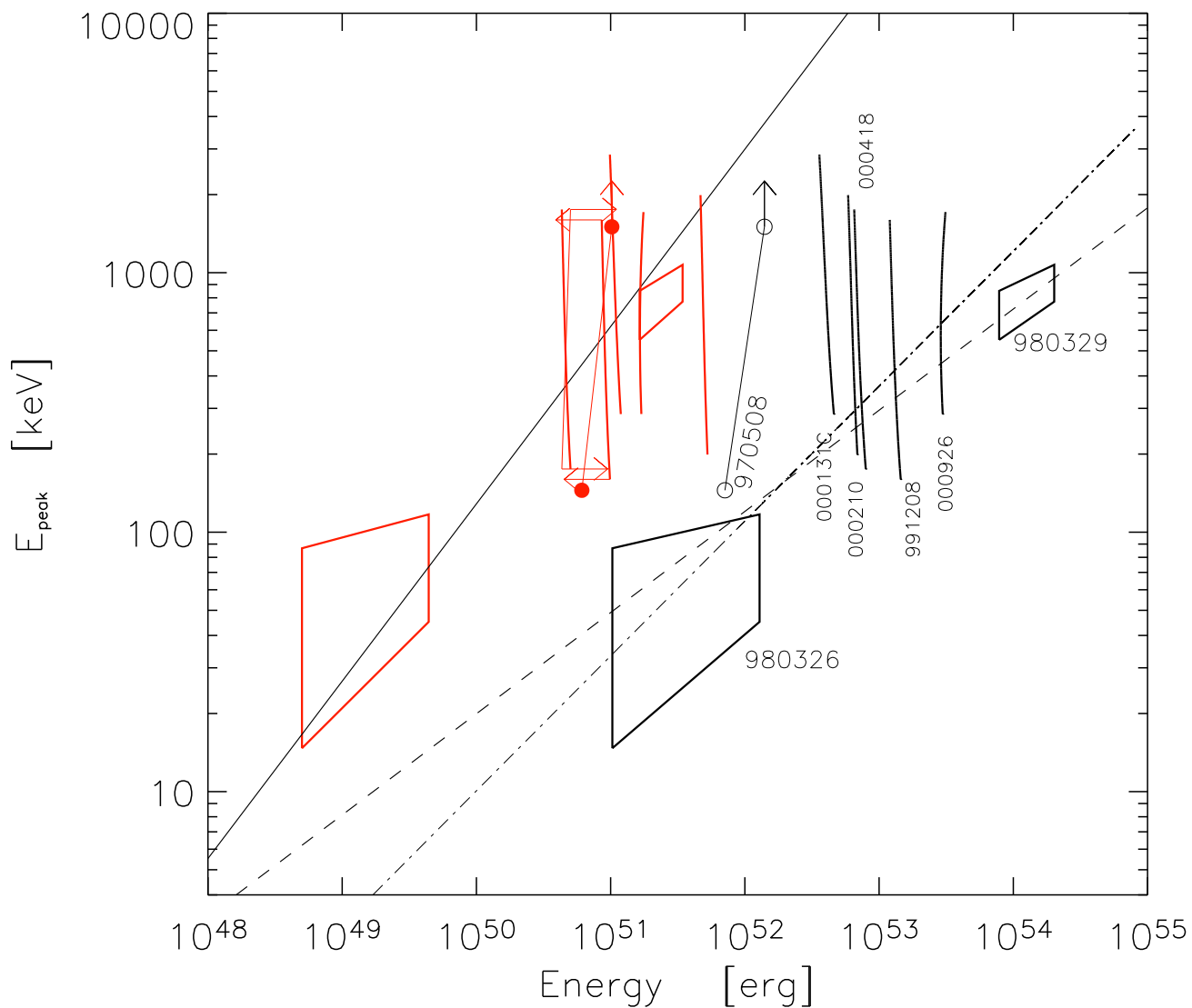


Fig. 3.— Rest frame peak energy $E_{peak} = E_{peak}^{obs}(1+z)$ versus bolometric energy for the sample of GRBs reported in Tab. 3,4 and excluded from the larger sample due to (i) uncertain redshift (980329, 980326), (ii) uncertain peak energy (970508) or (iii) no published spectral information (991208, 000212, 000131C, 000418, 000926).